

Uncovering the History of Cosmic Inflation from Anomalies in Cosmic Microwave Background Spectra

Matteo Braglia^{1,2}, Xingang Chen³, and Dhiraj Kumar Hazra^{4,2}

¹ *Instituto de Fisica Teorica, Universidad Autonoma de Madrid, Madrid, 28049, Spain*

² *INAF/OAS Bologna, via Gobetti 101, I-40129 Bologna, Italy*

³ *Institute for Theory and Computation, Harvard-Smithsonian Center
for Astrophysics, 60 Garden Street, Cambridge, MA 02138, USA*

⁴ *The Institute of Mathematical Sciences, HBNI, CIT Campus, Chennai 600113, India **

We propose an inflationary primordial feature model that can explain both the large and small-scale anomalies in the currently measured cosmic microwave background anisotropy spectra, revealing a clip of adventurous history of the Universe during its primordial epoch. Although the model is currently statistically indistinguishable from the Standard Model, we show that future observations such as the Simons Observatory and LiteBIRD will complement each other in distinguishing the model differences due to their accurate E-mode polarization measurements, and the PICO mission, if funded, can put stringent constraints on all characteristic properties. The model predicts a signal of classical primordial standard clock, which can also be used to distinguish the inflation and alternative scenarios in a model-independent fashion.

Introduction. The inflation scenario [1–6] is the leading candidate theory for the primordial Universe that started the Big Bang. There are high hopes that this knowledge will be advanced more definitively with future astrophysical observations, and we will be able to answer the important questions such as: Can we rule out alternative scenarios to inflation, or vice versa, using experimental data? For inflation, besides the broad-brush picture that the Universe was dominated by a form of vacuum energy and expanding with acceleration, can we learn any details of the underlying model?

To meet these goals, information beyond the Standard Model of cosmology is necessary. A potential source of information that may provide valuable insights in these questions are signals of primordial features. (See [7–9] for reviews.) Primordial features are strongly-scale-dependent deviations from the otherwise approximately scale-invariant spectra of the primordial density perturbations. These spectra are being probed by a variety of observations that measure the large-scale distribution of various contents of the universe. So far, measurements of the cosmic microwave background (CMB) provide the most precise data about the power spectrum of the density perturbations [10, 11]. Although being consistent with a featureless power-law spectrum, the temperature and polarization spectra of CMB anisotropies exhibit several statistically marginal feature-like anomalies in both large and small scales [10, 11].

At large scales, a dip in the spectrum has been noticed around $\ell \sim 20$ since WMAP [10]. At small scales, there is an oscillatory feature near $\ell \sim 750$ in the Planck data [11, 12]. Most of the model-building efforts so far have been focused on addressing either one of these anomalies, because they have qualitatively different characters.

It is well-known that the large scale anomaly may be

explained by a step-like sharp feature in the inflationary potential [10, 13–17]. Since the wavelength of this dip in the k -space is similar to the value of its k -location, the starting point of the sharp feature sinusoidal running should be near the location of this dip. Its amplitude has to decay quickly towards smaller scales in order to agree with the data.

The small scale anomaly has several possible explanations. It might be due to a sharp feature signal, but since its wavelength is much shorter than the value of its k -location, the sinusoidal running has to start at a much larger scale [18]. It is unlikely that such a sharp feature shares the same origin as the large-scale dip, because, as mentioned, the amplitude of the latter starts out large but decays very quickly towards small scales. Another possible explanation [11] is the resonant feature [19–23], which can arise, for example, from periodic ripples in an inflationary potential. This explanation does not address the large-scale anomaly.

On the other hand, it has been noticed in [18, 24] that these two anomalous features may share the same origin through the classical primordial standard clock (CPSC) effect [25–27]. From a top-down model-building point of view, the inflaton trajectory is determined by low-energy valleys of a potential landscape formed by many fields. It is natural to expect that such a path may not be straight and smooth (namely, have sharp features), and to expect steep cliffs perpendicular to this path (namely, the existence of many massive fields). Sharp features may temporarily disturb the inflaton away from its eventual attractor trajectory, and during the recovery process from the disturbance, some massive fields may be excited temporarily, oscillating and decaying away after a few e -folds. In this picture, the disturbance generates the sharp feature signal as a candidate for the large-scale anomaly, and the oscillation of a massive field, being at a high

frequency, generates the resonant feature at small scales.

Despite this interesting possibility in the model building, very few explicit CPSC models have been constructed so far and compared with data, and the available models only address the small scale anomaly [18, 24]. A main reason is that it is challenging to efficiently bridge between complicated feature models and data. This is partly because certain aspects of feature-model predictions depend very sensitively on the background evolution of inflation models. Moreover, the comparison between multi-field feature models and data is complicated, due to intricate relations between model parameters and numerical predictions, and due to multi-modal posterior distributions of feature parameters in data analysis. The purpose of this work is to make a significant progress in this direction. The first part of the challenge may be turned into an advantage. As we will demonstrate, the sensitivity of the properties of primordial features on background evolution means that a precise measurement of these signals can tell us many details about the underlying model. Combination of the bottom-up approach, that examines the properties of the anomalies [10, 11], and the top-down approach, that classifies the phenomenological characters of different types of features [7], is often useful in putting various model ingredients into place. The second part of the challenge can be addressed using a recently developed methodological pipeline [28], which is able to efficiently compare numerical predictions of multi-field feature models with data.

As a main result of this Letter, we will present a best-fit candidate model that vividly describes how, during the initial moment of the Universe, the inflaton is rolling at the top of an adventurous potential which is nonetheless quite natural from the point of view of a landscape. The emerging picture is drastically different from that of a single-field slow-roll model, but the feature signals the model generates in the CMB are all small corrections. This illustrates the richness of the primordial feature signals and the prospects of learning the history of the primordial epoch from data.

There is still another reward if such a CPSC signal can be measured precisely. The resonant part of this signal (namely, the clock signal), induced by the oscillation of a massive field and taking a mostly model-independent form, directly measures the scale factor of the primordial Universe as a function of time [18, 24–27], which is the defining property of a primordial universe scenario and can be used to rule out alternative scenarios in a model-independent fashion.

A nice future prospect of these feature signals is that the models have strictly correlated predictions in the polarization spectra of CMB. There are several ongoing (e.g. BICEP/Keck Array [29]) and forthcoming experiments (e.g. Simons Observatory [30], LiteBIRD [31], PICO [32], CMB S4 [33]) in the following decade that will measure the polarization of CMB with unprecedented

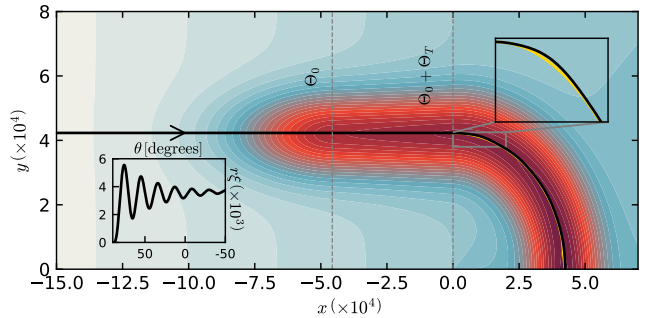


FIG. 1: A birdseye example of background trajectory in our model, plotted over equipotential surfaces (redder means lower potential). In terms of the Cartesian coordinates x and y shown here, for $x < 0$ the Θ and σ are Cartesian with $x = \Theta - (\Theta_T + \Theta_0)$ and $y = \sigma + \xi^{-1}$; while for $x > 0$ the Θ and σ become radial coordinates as in [35, 36] with $r = \sigma + \xi^{-1}$ and $\theta = \pi/2 - \xi(\Theta - \Theta_0 - \Theta_T)$. The insets show how the inflaton overshoots the bottom of the valley (yellow line) and climbs onto a side of the cliff [top-right], and the clock oscillation [bottom-left].

precisions. We forecast the prospects of the Simons Observatory (SO), LiteBIRD, and PICO in constraining the feature models, using as fiducial our best-fit CMB spectra.

The model. As summarized in [18, 25], in general there are two simple requirements for a model to be qualified as a CPSC model. First, there should be two observable stages of inflation connected by a sharp feature. Second, the sharp feature classically excites a massive field. The most model-dependent part of the full CPSC signal is the amplitude of the sharp feature signal and its smooth connection to the clock signal. We will use a step potential as part of the sharp feature. In two-field models and to connect with the oscillation of a massive field, the placement of this step in model configuration is also crucial and could lead to very different signals. Our model is described by the following Lagrangian,

$$\mathcal{L} = -\frac{1}{2}[1 + \Xi(\Theta)\sigma]^2(\partial\Theta)^2 - \frac{1}{2}(\partial\sigma)^2 - V(\Theta, \sigma), \quad (1)$$

where the potential $V(\Theta, \sigma)$ takes the following form [34],

$$V(\Theta, \sigma) = V_{\text{inf}} \left\{ 1 - \frac{1}{2}C_\Theta\Theta^2 + C_\sigma \left[1 - \exp\left(-\frac{(\Theta - \Theta_0)^2}{\Theta_f^2} \text{Heav}(\Theta - \Theta_0) - \frac{\sigma^2}{\sigma_f^2}\right) \right] \right\} \quad (2)$$

and $\Xi(\Theta) = \xi \text{Heav}(\Theta - \Theta_0 - \Theta_T)$.

This Lagrangian describes a two-field inflation model in which the field Θ is the inflationary direction and σ a field orthogonal to Θ . Despite of the slightly evolved mathematical expressions, the potential V and coupling Ξ are used to model the simple geometric configuration illustrated in Fig. 1. The evolutionary history of the inflaton is described as follows.

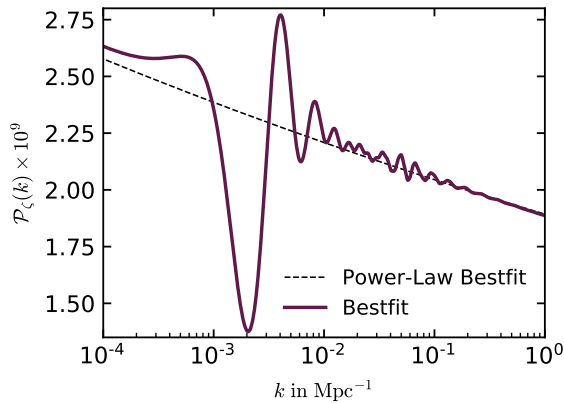


FIG. 2: The PPS of the bestfit model with the effective parameters: $V_{\text{inf}} = 5.45 \times 10^{-14}$, $C_{\Theta} = 0.0189$, $C_{\sigma} = 3.15 \times 10^{-8}$, $C_{\sigma}/\Theta_f^2 = 0.495$, $m_{\sigma}/H = 18.5$, $\xi\sigma_f = 0.0580$, $N_T = 1.17$, $N_0 = 14.38$. We used the convention $M_{\text{Pl}} = 1$. These gives $\Delta P_{\zeta}|_{\text{dip}}/P_{\zeta 0} \simeq 0.28$ and $\Delta P_{\zeta}|_{\text{clock}}/P_{\zeta 0} \simeq 0.038$. In this model, $k_0 \approx 6.66 \times 10^{-4} \text{Mpc}^{-1}$, corresponding to the bottom of the dip located at $k_{\text{dip}} \approx 2 \times 10^{-3} \text{Mpc}^{-1}$ or equivalently $\ell_{\text{dip}} \sim 20$; and $k_r \approx 4.38 \times 10^{-2} \text{Mpc}^{-1}$ or $\ell_{\text{clock}} \sim 600$.

During the first stage of inflation, the inflaton is rolling at the top of a plateau (which could also be a valley), until it encounters a cliff, which is located at $\Theta = \Theta_0$ and has the height and width determined by C_{σ} and Θ_f , and falls into a lower valley. In the two-field space, the path at the bottom of the lower valley starts out straight and begins to curve after a distance Θ_T . At the entrance of the curved path, the inflaton overshoots the bottom of the valley and climbs onto a side of the cliff, exciting the oscillation of a massive field. Due to the Hubble friction, the oscillation gradually decays and the inflaton settles down in the second stage of inflation.

Numerical results and effective parameters. We follow the methodology of Ref. [28] and directly compare numerical results on power spectrum with data.

A typical example of the primordial power spectrum (PPS) from this model is shown in Fig. 2. Note that there are two kinds of characteristically different running behaviors at large and small scales, respectively. At the large scales $k < k_r$, there is the sharp feature signal with its signature sinusoidal running $\sim \sin(2k/k_0 + \text{phase})$, which starts near $k = k_0$. At the small scales $k > k_r$, the clock signal starts to appear with its signature resonant running $\sim (\frac{2k}{k_r})^{-3/2} \sin(\frac{m_{\sigma}}{H} \ln \frac{2k}{k_r} + \text{phase})$. These properties are quite robust against model variations. On the other hand, the envelope of the sharp feature signal and its connection and relative amplitude to the clock signal are strongly model dependent, and play a crucial role in determining part of the model configuration.

As outlined in [28], when comparing a multi-parameter model with data, it is often convenient to first construct an equal number of effective parameters in terms of the model parameters. Each of these effective parameters

describes a distinct property of the feature signal in the power spectrum. The Lagrangian (1) contains eight model parameters. V_{inf} and C_{Θ} parameterize the scale of the inflationary potential and its slope, respectively. These two parameters are the same as those in the simplest single field model and no more transformation is needed. The other six parameters are as follows. Θ_0 , C_{σ} and Θ_f specify the location, depth and width of the step, respectively. σ_f describes the width of the trough, which together with some other parameters also determines the mass of the massive field σ . Θ_T gives the distance to the curved path, and $1/\xi$ is the radius of the curved path.

We first fix the slow-roll parameter ϵ to a small value, e.g. 10^{-7} , which determines the overall energy scale of the model. As long as ϵ is small, $\epsilon \lesssim 10^{-3}$, its value does not change the phenomenology of the model after proper rescalings of other parameters. The following is the identification of the effective parameters [37].

The depth of the dip feature in the PPS is determined by the height of the step

$$\frac{\Delta P_{\zeta}|_{\text{dip}}}{P_{\zeta 0}} \approx 1 - \left(1 + \frac{3C_{\sigma}}{\epsilon}\right)^{-1/2}, \quad (3)$$

and the extensiveness of the sinusoidal running is determined by the width of the step, $\Delta k \sim k_0 \sqrt{C_{\sigma}/\Theta_f^2}$.

These relations suggest two effective parameters: $\frac{\Delta P_{\zeta}|_{\text{dip}}}{P_{\zeta 0}}$ and C_{σ}/Θ_f^2 .

The amplitude of the clock signal, in addition to its running property mentioned previously, is determined by the initial velocity of the inflaton entering the curved path, the radius of the path and the mass of the σ -field:

$$\frac{\Delta P_{\zeta}|_{\text{clock}}}{P_{\zeta 0}} \Big|_{\text{amp}} \approx \frac{\sqrt{2\pi}}{3} \frac{\epsilon}{C_{\sigma}} (\xi\sigma_f)^2 \left(\frac{m_{\sigma}}{H}\right)^{1/2}, \quad (4)$$

where $m_{\sigma}/H \approx \sqrt{6C_{\sigma}}/\sigma_f$. This suggests two more effective parameters, $\log_{10} m_{\sigma}/H$ and $\frac{\Delta P_{\zeta}|_{\text{clock}}}{P_{\zeta 0}}$.

The transition between the step and the curved path is most conveniently described by the number of e -folds the inflaton spends in-between, $N_T \approx (\Theta_T/\sigma_f)(H/m_{\sigma})$, which we use as another effective parameter.

The last effective parameter is the overall k -location of the feature, which we parameterize as N_0 , defined as the e -fold from the beginning of inflation, at which the inflaton crosses the location of the step $\Theta(N_0) \equiv \Theta_0$ [38].

In total, the power spectrum is specified by eight parameters, which is six more than that in the Standard Model. In term of effective parameters, the starting locations of sharp feature and clock signal, k_0 and k_r , are related by $k_r \approx \exp(N_T) \frac{m_{\sigma}}{H} k_0$.

Data comparison and best fit. Our data analysis is based on publicly available latest Planck data of CMB temperature and E-mode polarization. Following the Planck inflation paper [11], we use

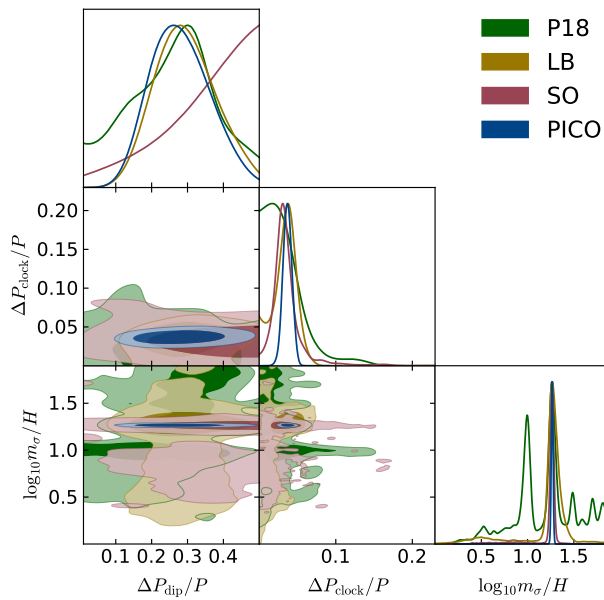


FIG. 3: Constraints from P18 and projected constraints on the parameters characterizing the amplitude of the dip and the amplitude and frequency of the clock signal.

`commander_dx12_v3.2.29` for temperature anisotropies and `small_100x143_offlike5_EE_Aplanck.B` for E-modes, both at $\ell = 2 - 29$; whereas we use the unbinned Plik `bin1` likelihood for TT, TE, EE anisotropies at high- ℓ . We refer to this dataset as P18.

Multi-modality of the posterior distributions of the feature parameters is expected as we had experienced in [28]. Therefore we use nested sampling through the PolyChord [39–41] implementation in CosmoMC [42]. From the samples in the data analysis, we plot the posterior distributions of the parameters and importantly, compute the Bayesian evidence or the marginal likelihood Z_i of the model i . The latter helps us compare our model to the featureless, baseline model.

Together with the cosmological parameters, i.e. $\omega_b, \omega_c, \tau_{\text{reio}}$ and $100 * \theta_s$, we vary the inflationary parameters as well as the nuisance parameters. The priors for the effective parameters are chosen as follows: $\log_{10} P_{C^*} \in [-8.82, -8.1]$, $C_\Theta \in [0.002, 0.04]$, $N_0 \in [13, 15.5]$, $\frac{\Delta P_{C^*}^{\text{dip}}}{P_{C^*}} \in [0, 0.5]$, $C_\sigma / \Theta_f^2 \in [0, 2.5]$, $N_T \in [0, 1.2]$, $\log_{10} m_\sigma / H \in [0, \log_{10} 75]$, $\frac{\Delta P_{C^*}^{\text{clock}}}{P_{C^*}} \in [0, 0.35]$. With these choices, the locations of both the dip feature and the clock signal are allowed to appear in the whole range of multipoles probed by Planck.

Planck constraints from our analysis are shown in grey in Fig. 3. Here, we focus on the parameters describing the feature amplitudes and the frequency of the clock signal. Full triangle plots showing constraints on all parameters will be presented in a companion paper [37]. Although our CPSC model does provide a better fit compared to the baseline model, the broad

contours indicate that current measurements of CMB anisotropies are not able to constrain our model and only give upper bounds on the amplitude of the large and small scale features. Consequently, the Bayes factor is $\ln B \equiv \ln(Z_{\text{feature}}/Z_{\text{featureless}}) = -0.13 \pm 0.38$, showing a weak preference (according to the Jeffreys’ scale [43]) for the baseline model and confirming no evidence of features in Planck data, consistent with previous analysis [11, 28].

However, a clear peak around $m_\sigma/H \sim 18$ stands out in the posterior. From the analysis of the samples we observe that almost all the better likelihood points concentrate around that mode. Using the BOBYQA algorithm [44], we obtain the bestfit candidate and quantify the improvement in the fit to P18 [45]. Our bestfit candidate’s PPS is presented in Fig. 2 and the corresponding CMB residuals in Fig. 4. The $\Delta\chi^2 = 19.8$ improvement over the featureless model is striking, with the dip feature fitting the low- ℓ data ($\Delta\chi_{\text{low-T}}^2 = 5.34$ and $\Delta\chi_{\text{low-E}}^2 = 1.11$) and the other properties, mostly the clock signal, fitting high- ℓ ($\Delta\chi_{\text{high-}\ell}^2 = 13.31$).

The improvement in fit can be appreciated by looking at the residual plot in Fig. 4, which clearly shows that the improvement is driven not only by the better fit to the dip in the TT residuals around $\ell \sim 20$, but also by the sinusoidal running of the sharp feature signal and, in particular, the clock signal. The clock signal oscillation, which starts around $\ell \gtrsim 600$, addresses the dip followed by a bump in the TT residuals around $\ell \sim 750$ and the associated feature in the TE residuals. The sinusoidal running part of the sharp feature signal also provides some weaker improvement in fits to the bump in the EE residuals around $\ell \sim 60$ and the dip around $\ell \sim 350$.

Forecast with CMB polarization. Assuming the $\mathcal{D}_\ell^{\text{TT}}, \mathcal{D}_\ell^{\text{EE}}, \mathcal{D}_\ell^{\text{TE}}$ from the best fit as the fiducial angular power spectra, using the projected noise power spectra from the upcoming LiteBIRD, SO and the PICO mission concept, we forecast future constraints on our model. LiteBIRD is a full sky CMB mission with a sensitivity of $2.2\mu\text{K} - \text{arcmin}$ in polarization and 0.5° resolution. SO is a ground based observation with a polarization noise an order of magnitude lower than Planck (which was $\sim 52\mu\text{K}$). While SO covers 40% of the sky (compared to 70% by LiteBIRD), it has a much finer resolution (better than $3'$). PICO is a NASA funded study for a CMB space mission with arcminute resolution and $0.65\mu\text{K} - \text{arcmin}$ polarization sensitivity. We compute the T and E noise levels using the beam functions and sensitivity in detectors following [46, 47] and use the SO noise for the Large Aperture Telescope baseline configuration [30]. We use the likelihood corresponding to an inverted Wishart distribution, as discussed in [48]. We use multipole ranges ($[\ell_{\text{min}} - \ell_{\text{max}}]$) $[2 - 1350]$, $[40 - 2500]$ and $[2 - 2500]$ for LiteBIRD, SO and PICO, respectively [49]. The projected error-bars for the three observations are plotted in Fig. 4. Using CosmoChord we project constraints on the parameters and plot them on top of the

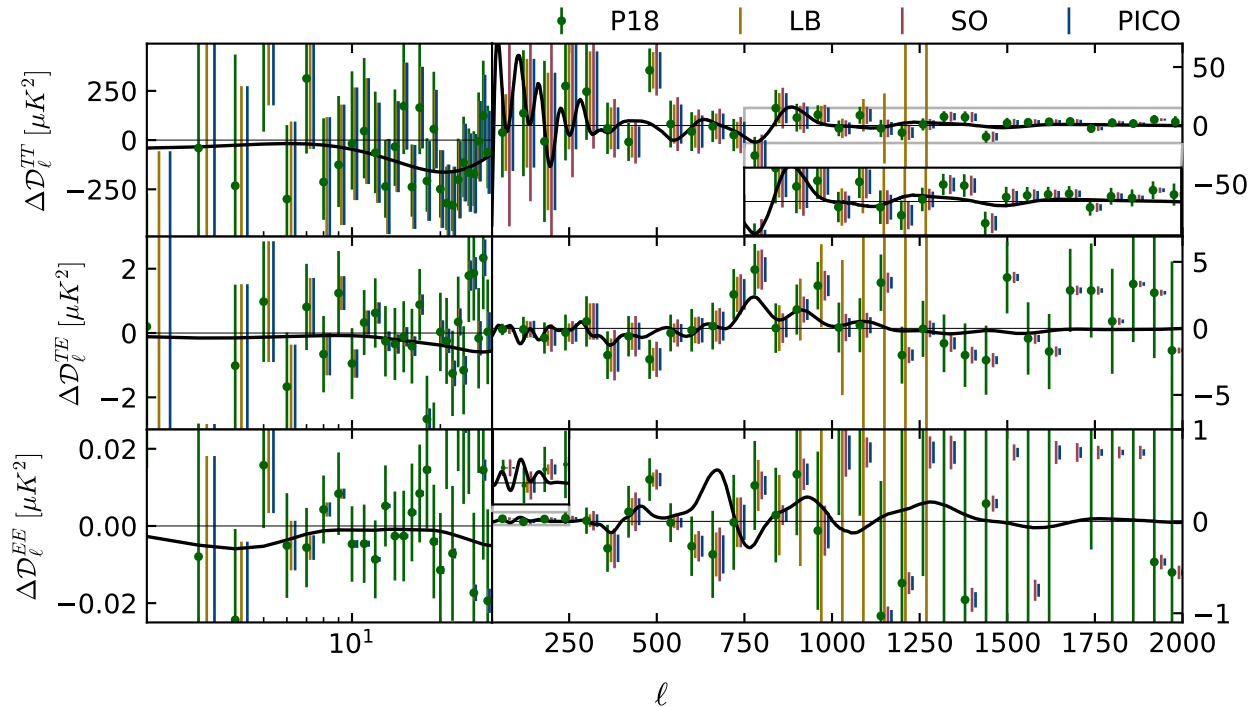


FIG. 4: Residual plots for our best fit candidate. P18 error bars are plotted in grey, whereas the forecast error bars for LiteBIRD, SO and PICO are plotted in light blue, orange and purple, respectively. Errors for $\ell > 30$ are binned with binwidth $\Delta\ell = 60$.

Planck constraints in Fig. 3.

These experiments will play complementary roles in constraining the model. The dip feature at large scales, and its subsequent sinusoidal running, are well constrained by LiteBIRD, but not by SO, which has a lower sky coverage. The clock signal on the other hand is better constrained by SO as LiteBIRD’s signal-to-noise decreases drastically at small scales due to wider beams. Since these two observations complement in constraining different aspects of the features, the intersection of the contours indicate the constraints expected in a joint analysis. Interestingly, PICO contours are even smaller than the intersecting region between LiteBIRD and SO. Given our assumption on the fiducial model, we find a projected Bayes factor of $\ln B \simeq 29$ [37], suggesting that a survey with similar configurations as PICO [50–52] will provide a decisive evidence in favor of or against our model. Restricting only to the small scale information from PICO ($\ell > 600$) [37], we find that PICO can also provide stringent constraints on the presence and frequency of the small scale clock signal, to test inflation against alternative scenarios.

Conclusions and discussions. CMB anomalies may hint at primordial physics beyond the standard scenario of single-field slow-roll inflation, which is characterized by a near scale-invariant spectrum of primordial fluctuations. In this letter, we have proposed a new classical standard clock model of inflation where a sharp feature

exciting massive-field oscillations addresses the low and mid- ℓ anomalies, whereas anomalies at high- ℓ are instead fitted by the clock signal itself. While the Bayesian evidence slightly favors a featureless spectrum, our model provides a much better fit to data. The improvement in the χ^2 for the global best fit candidate, characterized by a clock field with an effective mass ~ 18 times the Hubble scale of inflation, is as large as $\Delta\chi^2 \sim 19.8$. Assuming such a candidate as a fiducial cosmology, we have performed a forecast for future CMB experiments and highlighted the complementarity of measurements of E-mode spectra across different scales. In particular, LiteBIRD is able to measure the large-scale dip feature produced by our model, whereas the Simons observatory is able to measure some properties of the clock signal at smaller scales in the next few years. A futuristic all-scale cosmic-variance limited experiment such as PICO will provide strong evidence in favor of, or against, such features on a wider range of multipoles.

There are many other interesting aspects about the model-building and testing of primordial feature models such as the one presented in this work.

Besides signatures in CMB, primordial feature models also leave correlated imprints in the large-scale distributions of galaxies [53–62] and atomic hydrogen [63, 64], which will be further tested in future Large-Scale Structure and 21cm observations. Besides power spectrum, feature models also generate correlated signals in primor-

dial non-Gaussianities [19, 65–70]. It would be interesting to compute the bispectrum of this model and examine its observability.

As mentioned, the anomalies in the CMB power spectra can also be fit [11] by other inflationary models, including pure sharp feature models [13–17, 65, 71–74] and simple resonant models [19–23]. It is also possible that such features are generated by models of alternative scenarios to inflation [75, 76], or models containing non-standard primordial clocks [25, 77–79]. Our forecast on the size of error bars from future CMB polarization experiments offers some optimistic notes on the prospects of experimentally distinguishing many of these different cases if the amplitude of the signal is similar to that of the best-fit model in this Letter, although these aspects deserve to be studied more extensively.

All these add to the exciting prospects of probing the history of the primordial Universe using data from near future observations.

Acknowledgment. We thank Karim Benabed, Steven Gratton, John Kovac, Umberto Natale and Daniela Saadeh for very helpful discussions. Computations were run on the FASRC Cannon cluster at Harvard University. MB is supported by the Atracción de Talento contract no. 2019-T1/TIC-13177 granted by the Comunidad de Madrid in Spain.

* Electronic address: matteo.braglia@csic.es,
xingang.chen@cfa.harvard.edu,
dhiraj@imsc.res.in

- [1] A. H. Guth, “The Inflationary Universe: A Possible Solution to the Horizon and Flatness Problems,” *Phys. Rev. D* **23**, 347-356 (1981) doi:10.1103/PhysRevD.23.347
- [2] A. D. Linde, “A New Inflationary Universe Scenario: A Possible Solution of the Horizon, Flatness, Homogeneity, Isotropy and Primordial Monopole Problems,” *Phys. Lett. B* **108**, 389-393 (1982) doi:10.1016/0370-2693(82)91219-9
- [3] A. Albrecht and P. J. Steinhardt, “Cosmology for Grand Unified Theories with Radiatively Induced Symmetry Breaking,” *Phys. Rev. Lett.* **48**, 1220-1223 (1982) doi:10.1103/PhysRevLett.48.1220
- [4] A. A. Starobinsky, “A New Type of Isotropic Cosmological Models Without Singularity,” *Phys. Lett. B* **91**, 99-102 (1980) doi:10.1016/0370-2693(80)90670-X
- [5] K. Sato, “First Order Phase Transition of a Vacuum and Expansion of the Universe,” *Mon. Not. Roy. Astron. Soc.* **195**, 467-479 (1981) NORDITA-80-29.
- [6] V. F. Mukhanov and G. V. Chibisov, “Quantum Fluctuations and a Nonsingular Universe,” *JETP Lett.* **33**, 532-535 (1981)
- [7] X. Chen, “Primordial Non-Gaussianities from Inflation Models,” *Adv. Astron.* **2010**, 638979 (2010) doi:10.1155/2010/638979 [[arXiv:1002.1416](https://arxiv.org/abs/1002.1416) [astro-ph.CO]].
- [8] J. Chluba, J. Hamann and S. P. Patil, “Features and New Physical Scales in Primordial Observables: Theory and Observation,” *Int. J. Mod. Phys. D* **24**, no.10, 1530023 (2015) doi:10.1142/S0218271815300232 [[arXiv:1505.01834](https://arxiv.org/abs/1505.01834) [astro-ph.CO]].
- [9] A. Slosar, K. N. Abazajian, M. Abidi, P. Adshead, Z. Ahmed, D. Alonso, M. A. Amin, B. Ansarinejad, R. Armstrong and C. Baccigalupi, *et al.* “Scratches from the Past: Inflationary Archaeology through Features in the Power Spectrum of Primordial Fluctuations,” [[arXiv:1903.09883](https://arxiv.org/abs/1903.09883) [astro-ph.CO]].
- [10] H. V. Peiris *et al.* [WMAP], “First year Wilkinson Microwave Anisotropy Probe (WMAP) observations: Implications for inflation,” *Astrophys. J. Suppl.* **148**, 213-231 (2003) doi:10.1086/377228 [[arXiv:astro-ph/0302225](https://arxiv.org/abs/astro-ph/0302225) [astro-ph]].
- [11] Y. Akrami *et al.* [Planck], “Planck 2018 results. X. Constraints on inflation,” *Astron. Astrophys.* **641**, A10 (2020) doi:10.1051/0004-6361/201833887 [[arXiv:1807.06211](https://arxiv.org/abs/1807.06211) [astro-ph.CO]].
- [12] D. K. Hazra, A. Shafieloo and T. Souradeep, “Primordial power spectrum from Planck,” *JCAP* **11** (2014), 011 doi:10.1088/1475-7516/2014/11/011 [[arXiv:1406.4827](https://arxiv.org/abs/1406.4827) [astro-ph.CO]].
- [13] J. A. Adams, B. Cresswell and R. Easther, “Inflationary perturbations from a potential with a step,” *Phys. Rev. D* **64**, 123514 (2001) doi:10.1103/PhysRevD.64.123514 [[arXiv:astro-ph/0102236](https://arxiv.org/abs/astro-ph/0102236) [astro-ph]].
- [14] R. Bean, X. Chen, G. Hailu, S. H. H. Tye and J. Xu, “Duality Cascade in Brane Inflation,” *JCAP* **03**, 026 (2008) doi:10.1088/1475-7516/2008/03/026 [[arXiv:0802.0491](https://arxiv.org/abs/0802.0491) [hep-th]].
- [15] D. K. Hazra, M. Aich, R. K. Jain, L. Sriramkumar and T. Souradeep, “Primordial features due to a step in the inflaton potential,” *JCAP* **10**, 008 (2010) doi:10.1088/1475-7516/2010/10/008 [[arXiv:1005.2175](https://arxiv.org/abs/1005.2175) [astro-ph.CO]].
- [16] D. K. Hazra, A. Shafieloo, G. F. Smoot and A. A. Starobinsky, “Wiggly Whipped Inflation,” *JCAP* **08**, 048 (2014) doi:10.1088/1475-7516/2014/08/048 [[arXiv:1405.2012](https://arxiv.org/abs/1405.2012) [astro-ph.CO]].
- [17] V. Miranda, W. Hu and C. Dvorkin, “Polarization Predictions for Inflationary CMB Power Spectrum Features,” *Phys. Rev. D* **91**, no.6, 063514 (2015) doi:10.1103/PhysRevD.91.063514 [[arXiv:1411.5956](https://arxiv.org/abs/1411.5956) [astro-ph.CO]].
- [18] X. Chen, M. H. Namjoo and Y. Wang, “Models of the Primordial Standard Clock,” *JCAP* **02**, 027 (2015) doi:10.1088/1475-7516/2015/02/027 [[arXiv:1411.2349](https://arxiv.org/abs/1411.2349) [astro-ph.CO]].
- [19] X. Chen, R. Easther and E. A. Lim, “Generation and Characterization of Large Non-Gaussianities in Single Field Inflation,” *JCAP* **04**, 010 (2008) doi:10.1088/1475-7516/2008/04/010 [[arXiv:0801.3295](https://arxiv.org/abs/0801.3295) [astro-ph]].
- [20] R. Flauger, L. McAllister, E. Pajer, A. Westphal and G. Xu, “Oscillations in the CMB from Axion Monodromy Inflation,” *JCAP* **06**, 009 (2010) doi:10.1088/1475-7516/2010/06/009 [[arXiv:0907.2916](https://arxiv.org/abs/0907.2916) [hep-th]].
- [21] R. Flauger and E. Pajer, “Resonant Non-Gaussianity,” *JCAP* **01**, 017 (2011) doi:10.1088/1475-7516/2011/01/017 [[arXiv:1002.0833](https://arxiv.org/abs/1002.0833) [hep-th]].
- [22] X. Chen, “Folded Resonant Non-Gaussianity in General Single Field Inflation,” *JCAP* **12**, 003 (2010) doi:10.1088/1475-7516/2010/12/003 [[arXiv:1008.2485](https://arxiv.org/abs/1008.2485) [hep-th]].
- [23] M. Aich, D. K. Hazra, L. Sriramkumar and T. Souradeep,

- “Oscillations in the inflaton potential: Complete numerical treatment and comparison with the recent and forthcoming CMB datasets,” *Phys. Rev. D* **87**, 083526 (2013) doi:10.1103/PhysRevD.87.083526 [arXiv:1106.2798 [astro-ph.CO]].
- [24] X. Chen and M. H. Namjoo, “Standard Clock in Primordial Density Perturbations and Cosmic Microwave Background,” *Phys. Lett. B* **739**, 285-292 (2014) doi:10.1016/j.physletb.2014.11.002 [arXiv:1404.1536 [astro-ph.CO]].
- [25] X. Chen, “Primordial Features as Evidence for Inflation,” *JCAP* **01**, 038 (2012) doi:10.1088/1475-7516/2012/01/038 [arXiv:1104.1323 [hep-th]].
- [26] X. Chen, “Fingerprints of Primordial Universe Paradigms as Features in Density Perturbations,” *Phys. Lett. B* **706**, 111-115 (2011) doi:10.1016/j.physletb.2011.11.009 [arXiv:1106.1635 [astro-ph.CO]].
- [27] X. Chen and C. Ringeval, “Searching for Standard Clocks in the Primordial Universe,” *JCAP* **08**, 014 (2012) doi:10.1088/1475-7516/2012/08/014 [arXiv:1205.6085 [astro-ph.CO]].
- [28] M. Braglia, X. Chen and D. K. Hazra, “Comparing multi-field primordial feature models with the Planck data,” *JCAP* **06**, 005 (2021) doi:10.1088/1475-7516/2021/06/005 [arXiv:2103.03025 [astro-ph.CO]].
- [29] L. Monceli, P. A. R. Ade, Z. Ahmed, M. Amiri, D. Barkats, R. Basu Thakur, C. A. Bischoff, J. J. Bock, V. Buza and J. Cheshire, *et al.* “Receiver development for BICEP Array, a next-generation CMB polarimeter at the South Pole,” *Proc. SPIE Int. Soc. Opt. Eng.* **11453**, 1145314 (2020) doi:10.1117/12.2561995 [arXiv:2012.04047 [astro-ph.IM]].
- [30] P. Ade *et al.* [Simons Observatory], “The Simons Observatory: Science goals and forecasts,” *JCAP* **02**, 056 (2019) doi:10.1088/1475-7516/2019/02/056 [arXiv:1808.07445 [astro-ph.CO]].
- [31] M. Hazumi *et al.* [LiteBIRD], “LiteBIRD: JAXA’s new strategic L-class mission for all-sky surveys of cosmic microwave background polarization,” *Proc. SPIE Int. Soc. Opt. Eng.* **11443** (2020), 114432F doi:10.1117/12.2563050 [arXiv:2101.12449 [astro-ph.IM]].
- [32] S. Hanany *et al.* [NASA PICO], “PICO: Probe of Inflation and Cosmic Origins,” [arXiv:1902.10541 [astro-ph.IM]].
- [33] K. Abazajian, G. Addison, P. Adshead, Z. Ahmed, S. W. Allen, D. Alonso, M. Alvarez, A. Anderson, K. S. Arnold and C. Baccigalupi, *et al.* “CMB-S4 Science Case, Reference Design, and Project Plan,” [arXiv:1907.04473 [astro-ph.IM]].
- [34] In order not to make confusion with the field Θ we denote the Heaviside Theta function by Heav .
- [35] X. Chen and Y. Wang, “Large non-Gaussianities with Intermediate Shapes from Quasi-Single Field Inflation,” *Phys. Rev. D* **81**, 063511 (2010) doi:10.1103/PhysRevD.81.063511 [arXiv:0909.0496 [astro-ph.CO]].
- [36] X. Chen and Y. Wang, “Quasi-Single Field Inflation and Non-Gaussianities,” *JCAP* **04**, 027 (2010) doi:10.1088/1475-7516/2010/04/027 [arXiv:0911.3380 [hep-th]].
- [37] M. Braglia, X. Chen and D. K. Hazra, [arXiv:2108.10110 [astro-ph.CO]].
- [38] We choose $k = 0.05 \text{ Mpc}^{-1}$ for the mode that exits the horizon 50 e -folds towards the end of the inflation. We fix a total of 68 e -folds.
- [39] <https://github.com/PolyChord>
- [40] W. J. Handley, M. P. Hobson and A. N. Lasenby, “PolyChord: nested sampling for cosmology,” *Mon. Not. Roy. Astron. Soc.* **450**, no.1, L61-L65 (2015) doi:10.1093/mnras/slv047 [arXiv:1502.01856 [astro-ph.CO]].
- [41] W. J. Handley, M. P. Hobson and A. N. Lasenby, “polychord: next-generation nested sampling,” *Mon. Not. Roy. Astron. Soc.* **453**, no.4, 4385-4399 (2015) doi:10.1093/mnras/stv1911 [arXiv:1506.00171 [astro-ph.IM]].
- [42] A. Lewis and S. Bridle, “Cosmological parameters from CMB and other data: A Monte Carlo approach,” *Phys. Rev. D* **66**, 103511 (2002) doi:10.1103/PhysRevD.66.103511 [arXiv:astro-ph/0205436 [astro-ph]].
- [43] R. E. Kass and A. E. Raftery, “Bayes Factors,” *J. Am. Statist. Assoc.* **90**, no.430, 773-795 (1995) doi:10.1080/01621459.1995.10476572
- [44] M. Powell, “The BOBYQA Algorithm for Bound Constrained Optimization without Derivatives,” Technical Report, Department of Applied Mathematics and Theoretical Physics.
- [45] Note that we vary cosmological and inflationary parameters in our best-fit analysis and, in order to be conservative, also the nuisance parameters. Here we also include the χ^2 for the priors in the foreground and calibration parameters. See method-III in Sec. 2.5.2 of Ref. [28] for details.
- [46] L. Knox, “Determination of inflationary observables by cosmic microwave background anisotropy experiments,” *Phys. Rev. D* **52** (1995), 4307-4318 doi:10.1103/PhysRevD.52.4307 [arXiv:astro-ph/9504054 [astro-ph]].
- [47] M. Tegmark, “CMB mapping experiments: A Designer’s guide,” *Phys. Rev. D* **56** (1997), 4514-4529 doi:10.1103/PhysRevD.56.4514 [arXiv:astro-ph/9705188 [astro-ph]].
- [48] S. Hamimeche and A. Lewis, “Likelihood Analysis of CMB Temperature and Polarization Power Spectra,” *Phys. Rev. D* **77** (2008), 103013 doi:10.1103/PhysRevD.77.103013 [arXiv:0801.0554 [astro-ph]].
- [49] A detailed discussion on the forecast analysis is available in [37].
- [50] K. Young, M. Alvarez, N. Battaglia, J. Bock, J. Borrill, D. Chuss, B. Crill, J. Delabrouille, M. Devlin and L. Fissel, *et al.* “Optical Design of PICO, a Concept for a Space Mission to Probe Inflation and Cosmic Origins,” [arXiv:1808.01369 [astro-ph.IM]].
- [51] J. Delabrouille *et al.* [CORE], “Exploring cosmic origins with CORE: Survey requirements and mission design,” *JCAP* **04** (2018), 014 doi:10.1088/1475-7516/2018/04/014 [arXiv:1706.04516 [astro-ph.IM]].
- [52] <http://cmb-bharat.in/>
- [53] Z. Huang, L. Verde and F. Vernizzi, “Constraining inflation with future galaxy redshift surveys,” *JCAP* **04**, 005 (2012) doi:10.1088/1475-7516/2012/04/005 [arXiv:1201.5955 [astro-ph.CO]].
- [54] X. Chen, C. Dvorkin, Z. Huang, M. H. Namjoo and L. Verde, “The Future of Primordial Fea-

- tures with Large-Scale Structure Surveys,” JCAP **11**, 014 (2016) doi:10.1088/1475-7516/2016/11/014 [arXiv:1605.09365 [astro-ph.CO]].
- [55] M. Ballardini, F. Finelli, C. Fedeli and L. Moscardini, “Probing primordial features with future galaxy surveys,” JCAP **10**, 041 (2016) [erratum: JCAP **04**, E01 (2018)] doi:10.1088/1475-7516/2016/10/041 [arXiv:1606.03747 [astro-ph.CO]].
- [56] G. A. Palma, D. Sapone and S. Sypsas, “Constraints on inflation with LSS surveys: features in the primordial power spectrum,” JCAP **06**, 004 (2018) doi:10.1088/1475-7516/2018/06/004 [arXiv:1710.02570 [astro-ph.CO]].
- [57] B. L’Huillier, A. Shafieloo, D. K. Hazra, G. F. Smoot and A. A. Starobinsky, “Probing features in the primordial perturbation spectrum with large-scale structure data,” Mon. Not. Roy. Astron. Soc. **477**, no.2, 2503-2512 (2018) doi:10.1093/mnras/sty745 [arXiv:1710.10987 [astro-ph.CO]].
- [58] M. Ballardini, F. Finelli, R. Maartens and L. Moscardini, “Probing primordial features with next-generation photometric and radio surveys,” JCAP **04**, 044 (2018) doi:10.1088/1475-7516/2018/04/044 [arXiv:1712.07425 [astro-ph.CO]].
- [59] F. Beutler, M. Biagetti, D. Green, A. Slosar and B. Wallisch, “Primordial Features from Linear to Nonlinear Scales,” Phys. Rev. Res. **1**, no.3, 033209 (2019) doi:10.1103/PhysRevResearch.1.033209 [arXiv:1906.08758 [astro-ph.CO]].
- [60] M. Ballardini, R. Murgia, M. Baldi, F. Finelli and M. Viel, “Non-linear damping of superimposed primordial oscillations on the matter power spectrum in galaxy surveys,” JCAP **04**, no.04, 030 (2020) doi:10.1088/1475-7516/2020/04/030 [arXiv:1912.12499 [astro-ph.CO]].
- [61] I. Debono, D. K. Hazra, A. Shafieloo, G. F. Smoot and A. A. Starobinsky, “Constraints on features in the inflationary potential from future Euclid data,” Mon. Not. Roy. Astron. Soc. **496**, no.3, 3448-3468 (2020) doi:10.1093/mnras/staa1765 [arXiv:2003.05262 [astro-ph.CO]].
- [62] Y. Li, H. M. Zhu and B. Li, “Reconstructing features in the primordial power spectrum,” [arXiv:2102.09007 [astro-ph.CO]].
- [63] X. Chen, P. D. Meerburg and M. Münchmeyer, “The Future of Primordial Features with 21 cm Tomography,” JCAP **09**, 023 (2016) doi:10.1088/1475-7516/2016/09/023 [arXiv:1605.09364 [astro-ph.CO]].
- [64] Y. Xu, J. Hamann and X. Chen, “Precise measurements of inflationary features with 21 cm observations,” Phys. Rev. D **94**, no.12, 123518 (2016) doi:10.1103/PhysRevD.94.123518 [arXiv:1607.00817 [astro-ph.CO]].
- [65] X. Chen, R. Easther and E. A. Lim, “Large Non-Gaussianities in Single Field Inflation,” JCAP **06**, 023 (2007) doi:10.1088/1475-7516/2007/06/023 [arXiv:astro-ph/0611645 [astro-ph]].
- [66] P. Adshead, C. Dvorkin, W. Hu and E. A. Lim, “Non-Gaussianity from Step Features in the Inflationary Potential,” Phys. Rev. D **85**, 023531 (2012) doi:10.1103/PhysRevD.85.023531 [arXiv:1110.3050 [astro-ph.CO]].
- [67] D. K. Hazra, L. Sriramkumar and J. Martin, “BINGO: A code for the efficient computation of the scalar bispectrum,” JCAP **05**, 026 (2013) doi:10.1088/1475-7516/2013/05/026 [arXiv:1201.0926 [astro-ph.CO]].
- [68] N. Bartolo, D. Cannone and S. Matarrese, “The Effective Field Theory of Inflation Models with Sharp Features,” JCAP **10**, 038 (2013) doi:10.1088/1475-7516/2013/10/038 [arXiv:1307.3483 [astro-ph.CO]].
- [69] J. R. Fergusson, H. F. Gruetjen, E. P. S. Shellard and M. Liguori, “Combining power spectrum and bispectrum measurements to detect oscillatory features,” Phys. Rev. D **91**, no.2, 023502 (2015) doi:10.1103/PhysRevD.91.023502 [arXiv:1410.5114 [astro-ph.CO]].
- [70] J. R. Fergusson, H. F. Gruetjen, E. P. S. Shellard and B. Wallisch, “Polyspectra searches for sharp oscillatory features in cosmic microwave sky data,” Phys. Rev. D **91**, no.12, 123506 (2015) doi:10.1103/PhysRevD.91.123506 [arXiv:1412.6152 [astro-ph.CO]].
- [71] A. A. Starobinsky, “Spectrum of adiabatic perturbations in the universe when there are singularities in the inflation potential,” JETP Lett. **55**, 489-494 (1992)
- [72] A. Achúcarro, J. O. Gong, S. Hardeman, G. A. Palma and S. P. Patil, “Features of heavy physics in the CMB power spectrum,” JCAP **01**, 030 (2011) doi:10.1088/1475-7516/2011/01/030 [arXiv:1010.3693 [hep-ph]].
- [73] X. Gao, D. Langlois and S. Mizuno, “Influence of heavy modes on perturbations in multiple field inflation,” JCAP **10**, 040 (2012) doi:10.1088/1475-7516/2012/10/040 [arXiv:1205.5275 [hep-th]].
- [74] G. Cañas-Herrera, J. Torrado and A. Achúcarro, “Bayesian reconstruction of the inflaton’s speed of sound using CMB data,” [arXiv:2012.04640 [astro-ph.CO]].
- [75] X. Chen, A. Loeb and Z. Z. Xianyu, “Unique Fingerprints of Alternatives to Inflation in the Primordial Power Spectrum,” Phys. Rev. Lett. **122**, no.12, 121301 (2019) doi:10.1103/PhysRevLett.122.121301 [arXiv:1809.02603 [astro-ph.CO]].
- [76] G. Domènech, X. Chen, M. Kamionkowski and A. Loeb, “Planck residuals anomaly as a fingerprint of alternative scenarios to inflation,” JCAP **10**, 005 (2020) doi:10.1088/1475-7516/2020/10/005 [arXiv:2005.08998 [astro-ph.CO]].
- [77] Q. G. Huang and S. Pi, “Power-law modulation of the scalar power spectrum from a heavy field with a monomial potential,” JCAP **04**, 001 (2018) doi:10.1088/1475-7516/2018/04/001 [arXiv:1610.00115 [hep-th]].
- [78] G. Domènech, J. Rubio and J. Wons, “Mimicking features in alternatives to inflation with interacting spectator fields,” Phys. Lett. B **790**, 263-269 (2019) doi:10.1016/j.physletb.2019.01.039 [arXiv:1811.08224 [astro-ph.CO]].
- [79] Y. Wang, Z. Wang and Y. Zhu, “Non-standard primordial clocks from induced mass in alternative to inflation scenarios,” JCAP **11**, 026 (2020) doi:10.1088/1475-7516/2020/11/026 [arXiv:2007.09677 [hep-th]].